

Synthesis and Physical Properties of Protein Core Mimetics

Jeffrey A. Turk and David B. Smithrud*

Department of Chemistry, University of Cincinnati, Cincinnati, Ohio 45221-0172

david.smithrud@uc.edu

Received July 9, 2001

A series of mimetic cores composed of a synthetic scaffold and amino acids have been constructed and their properties investigated in chloroform. A relative measure of H-bond strength was obtained by comparing temperature coefficients derived from variable-temperature ^1H NMR experiments. Although most templates had a strong H-bond, only a single template composed of D- and L-phenylalanines was able to form two strong H-bonds. Templates containing D- and L-leucines formed only a single H-bond. The results of these studies suggest that aromatic edge-to-face interactions provide greater stabilization energy than aliphatic–aromatic interactions in the tightly packed hydrophobic cores of proteins. Partial structures of the templates were derived by analyzing a series of two-dimensional ^1H NMR spectra and performing molecular mechanics calculations using AMBER and MMFF94 force fields.

Introduction

Protein cores contain a large proportion of aliphatic and aromatic residues that are tightly packed. Close packing of side chains maximizes their van der Waals interaction energy, which provides a large portion of the folding energy of proteins.¹ Besides being a fundamental property of proteins, understanding the intricate details of protein cores is necessary for creating de novo proteins.² One intriguing question about core properties is whether interactions between aromatic rings are more important in terms of energy or structure than those between aromatic rings and aliphatic side chains. Theoretical models have shown that electrostatic forces, which are not available for aliphatic side chains, guide aromatic alignment. These forces are thought to arise through a weak H-bond between the partially charged hydrogen atoms of one aromatic ring with the electron-rich face of another ring³ or through favorable σ – π attraction.⁴ The existence of electrostatic interactions is consistent with the fact that aromatic pairs prefer an edge-to-face (T-stacking) arrangement in proteins⁵ and in crystal structures of aromatic molecules.⁶ An off-set, face-to-face arrangement has been proposed to exist in the absorption spectrum of benzene.⁷ Monte Carlo simulations have correctly predicted that a T-stacked arrangement was the most stable. These studies, however, found that van der

Waals energies, and not electrostatic interactions, provided the driving force for the association of variously arranged aromatic pairs.⁸ Electrostatic terms were actually unfavorable or only slightly favorable, depending on the arrangement of the aromatic pair.

Only a small number of model systems have been created that examine the energies involved in T-stacked aromatic rings, and even fewer systems compare T-stacked energies against aliphatic–aromatic interactions. Benson has shown that T-stacking interactions between a porphyrin ring and the side chains of phenylalanine and tryptophan stabilized α -helix formation.⁹ A face-to-face arrangement of covalently linked phenyl rings was stabilized when their quadrupole moments of opposite signs were aligned, whereas interactions between rings composed of identical moments were destabilizing.¹⁰ Apparently, stacked aromatic rings prefer to have their quadrupole moments aligned, which suggests strongly that an additional electrostatic energy term exists in the interaction between aromatic rings. Mutational studies of proteins, however, showed that a single methyl group interacting with the face of Tyr provided about the same stabilization energy as the interaction between an aromatic pair (–1.9 and –1.3 kcal/mol, respectively).¹¹ Experimental results obtained by Wilcox, who created a unique molecular torsional balance designed to quantify the interaction energies between aromatic rings and between aromatic rings and aliphatic side chains, showed that these interactions have the same energy.¹² Computational modeling results of the torsional balance experi-

* To whom correspondence should be addressed. Fax: (513) 556-9239.

(1) Honig B.; Yang A. S. *Adv. Protein Chem.* **1995**, *46*, 27–58.
(2) (a) Hellings, H. W. *Proc. Natl. Acad. Sci. U.S.A.* **1997**, *94*, 10015–10017. (b) Richardson, J. S.; Richardson, D. C.; Tweedy, N. B.; Gernert, K. M.; Quinn, T. P.; Hecht, M. H.; Erickson, B. W.; Yan, Y. B.; McClain, R. D.; Donlan, M. E.; Surles, M. C. *Biophys. J.* **1992**, *63*, 1186–1209.
(3) Burley, S. K.; Petsko, G. A. *Adv. Protein Chem.* **1988**, *39*, 125–189.
(4) Hunter, C. A.; Sanders, J. K. M. *J. Am. Chem. Soc.* **1990**, *112*, 5525–5534.
(5) (a) Burley, S. K.; Petsko, G. A. *J. Am. Chem. Soc.* **1986**, *108*, 7995–8001. (b) Burley, S. K.; Petsko, G. A. *Science* **1985**, *229*, 23–28.
(6) Desiraju, G. R.; Gavezzotti, A. *J. Chem. Soc., Chem. Commun.* **1989**, 621–623.
(7) Law, K. S.; Schauer, M.; Bernstein, E. R. *J. Chem. Phys.* **1984**, *81*, 4871–4882.

(8) Jorgensen, W. L.; Severance, D. L. *J. Am. Chem. Soc.* **1990**, *112*, 4768–4774.

(9) Liu, D. H.; Williamson, D. A.; Kennedy, M. L.; Williams, T. D.; Morton, M. M.; Benson, D. R. *J. Am. Chem. Soc.* **1999**, *121*, 11798–11812.

(10) Heaton, N. J.; Bello, P.; Herradon, B.; del Campo, A.; Jimenez-Barbero, J. *J. Am. Chem. Soc.* **1998**, *120*, 12371–12384.

(11) (a) Serrano, L.; Bycroft, M.; Fersht, A. R. *J. Mol. Biol.* **1991**, *218*, 465–475. (b) Matouschek, A.; Kellis, J. T.; Serrano, L.; Fersht, A. R. *Nature (London)* **1989**, *340*, 122–126.

(12) Kim, E.; Paliwal, S.; Wilcox, C. S. *J. Am. Chem. Soc.* **1998**, *120*, 11192–11193.

ments¹³ supported Wilcox's conclusion that dispersion forces and not electrostatic interactions are dominant in T-stacked rings.

We have created a series of templates that systematically measure the interactions between aliphatic and aromatic amino acids in a protein-like core. The goals of these studies were to determine whether the alignment of aromatic or aliphatic side chains (structure) can affect H-bond formation (function) and whether aromatic interactions provided more structure and function than aliphatic–aromatic interactions. The hydrophobic core of the small $\beta\beta\alpha$ -motif observed in the Zif268 zinc finger protein was chosen as a model.¹⁴ The side chains of Tyr05 and Phe16 surround the side chain of Leu22 in zinc finger 1 to form a hydrophobic core. Accordingly, we have designed a two-tier template that combines glycine, L-phenylalanine, D-phenylalanine, L-leucine, or D-leucine to form mimetic cores. In this paper, the partial structures of the templates and the strength of their H-bonds are examined to provide some insights into the interactions that occur between side chains in the hydrophobic cores of proteins.

Results and Discussion

Template Design. Templates 1–6 (Table 1) were created to determine which combination of amino acids produces a core that stabilizes an H-bond in chloroform. To ensure that interaction energies in the core dominated template structure, the internal amides were alkylated. Removing these N-Hs eliminated the possibility of a seven-membered H-bonded ring forming between the internal amides. Having alkylated amides also reduced the number of H-bond donors, which lowered the number of possible template conformers and simplified the NMR spectra. To further simplify structure determination, the amino acids were added as either the *N*-methyl or *N*-ethyl amides. Besides reducing the number of N-H moieties for H-bond formation to two, the combination of a methyl and ethyl amide gave the templates asymmetry. Having dissimilar amino acids made it easier to identify the template's protons through two-dimensional NMR analysis. Even though the templates have only two N-H moieties, multiple H-bonded rings were still possible such as a 13-membered ring with the two terminal amides forming an H-bond, a 10-membered ring with one terminal amide forming an H-bond to the other internal amide's carbonyl oxygen atom, or a seven-membered ring where the amino acids fold back on themselves (Figure 1). The potential of forming multiple H-bonded rings made this template a convenient model system to determine if side-chain interactions can contribute to template structure and H-bond strength.

Synthesis of the Templates. The basic scaffold **7** was easily constructed through a Diels–Alder reaction between anthracene and maleic anhydride (Scheme 1).¹⁵ A Diels–Alder reaction of 1,3-cyclohexadiene and maleic anhydride¹⁶ provided the scaffold for template **1** (Table 1). Amino acid salts were prepared from the commercially available *N*-Boc-protected amino acids, which were *N*-

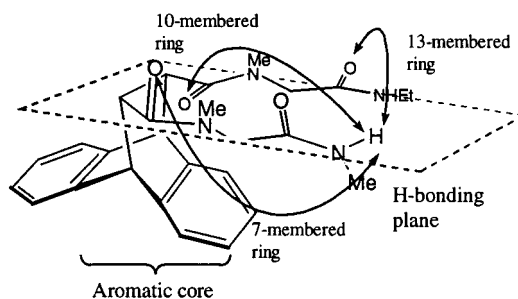
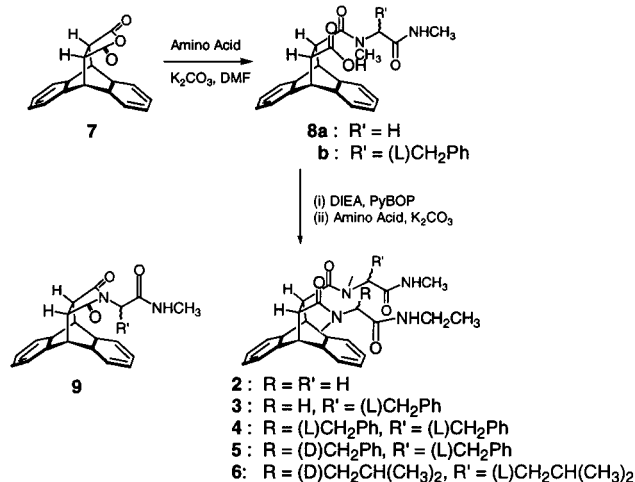


Figure 1. Basic template structure showing the aromatic core and the possible H-bonded rings that could form in the H-bonding plane.

Scheme 1



methylated¹⁷ and amidated¹⁸ following literature procedures. Opening of anhydride **7** in DMF, giving the amides **8a,b**, was achieved using the TFA salt of an amino acid derivative in the presence of K_2CO_3 . Activation of the resulting carboxylic acid with PyBOP,¹⁹ followed by the addition of the second derivatized amino acid, provided templates **1–6** either as a single species or a mixture of diastereomers, which were separated. It is noteworthy that activation of templates that contained nonmethylated internal amides generally resulted in the formation of the stable imide **9**,²⁰ which could not be converted to the desired diamino template. PyBOP was the only activating reagent that provided templates containing two amino acids that were not *N*-methylated.

H-Bond Strength Determination. A relative measure of hydrogen bond strength was obtained by comparing temperature coefficients of amide protons. Temperature coefficients are defined as the slopes of plots that correlate the changes in chemical shifts of protons with temperature (Note: H-bonded proton resonances shifted upfield with an increase in solution temperature, Figure 2).²¹ In chloroform, amide protons freely exposed to the solvent, i.e., not H-bonded, have temperature coefficients in the range of -2.4 to -3.5 ppb/K. N-H protons that remain hydrogen bonded in the experimen-

(13) Nakamura, K.; Houk, K. N. *Org. Lett.* **1999**, *1*, 2049–2051.

(14) Pavletich, N. P.; Pabo, C. O. *Science* **1991**, *252*, 809–817.

(15) Diels, O.; Alder, K. *Justus Liebigs Ann. Chem.* **1931**, *486*, 191–196.

(16) (a) Bergmann, E. D.; Shahak, I. *J. Chem. Soc.* **1959**, 1418–1422. (b) Alder, K.; Stein, G. *Ann.* **1933**, *504*, 224–257.

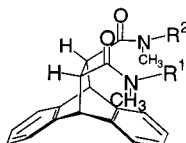
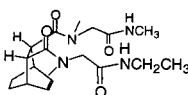
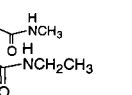
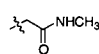
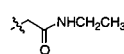
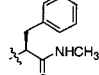
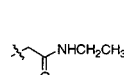
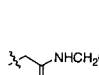
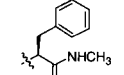
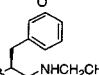
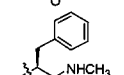
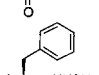
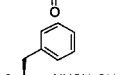
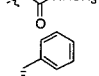
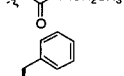
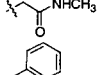
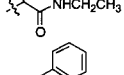
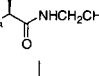
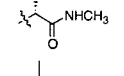
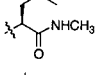
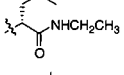
(17) Li, Wen-Ren; Peng, Shao-Zheng *Tetrahedron Lett.*, **1998**, *39*, 7373–7376.

(18) Hansen, T. K.; Ankersen, M.; Hansen, B.; Raun, K.; Nielsen, K. K. *J. Med. Chem.* **1998**, *41*, 3705–3714.

(19) Hibbs, D. E.; Hursthouse, M. B.; Jones, I. G.; Jones, W.; Abdul Malik, K. M.; North, M. *J. Org. Chem.* **1998**, *63*, 1496–1504.

(20) Edwin, W.; Stephan, F.; Ingeborg, C. *J. Org. Chem.* **1991**, *56*, 7281–7288.

Table 1. Temperature Dependencies for the ^1H NMR Resonances of N-H Protons in CDCl_3 at 298 K

				
Compound no.	R ¹	R ²	Temperature Coefficient ^a (Chemical Shift) ^b	
			Downfield NH	Upfield NH
1			-7.3 (6.81)	nb ^c (6.26)
2			-6.3 (6.53)	nb (6.20)
3a			-5.3 (6.39)	nb (6.15)
3b			-4.1 (6.58)	-4.2 (5.58)
4a			-6.0 (6.25)	nb (6.07)
4b			-6.0 (6.43)	nb (5.97)
5a			-6.5 (6.59)	-6.4 (6.41)
5b			nb (6.11)	nb (6.11)
6a			-5.7 (6.60)	nb (6.36)
6b			nb (6.12)	nb (6.11)

^a Units are ppb/K, uncertainties are ± 0.1 ppm/K. ^b Units are ppm, downfield and upfield refer to the relative chemical shifts of the two N-H protons. ^c nb means non-hydrogen-bonding N-H (temperature coefficient -2.5 to -3.5 ppb/K).

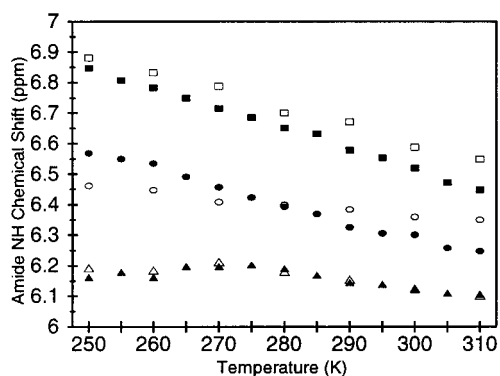


Figure 2. Representative plots of the temperature dependencies of the amide proton NMR chemical shifts for templates **5** and **6** that were used to derive temperature coefficients. \blacksquare = **5a** downfield N-H, \bullet = **5a** upfield N-H, \blacktriangle = **5b** both N-Hs, \square = **6a** downfield N-H, \circ = **6a** upfield N-H, \triangle = **6b** both N-Hs.

tal temperature range have values less negative than -2.4 ppb/K, whereas ones that undergo a transition from

a bound to an unbound state have values more negative than -3.5 ppb/K.²² For these latter protons, larger negative coefficients indicate a stronger H-bond. Studies in chloroform are convenient because the solvent does not compete strongly with H-bond formation, and we found that in chloroform, the number of template conformers was reduced. Most templates or at least one diastereomer formed a single intramolecular H-bond (Table 1).

A major exception was obtained for the diastereomers of template **5**. One diastereomer had two strong H-bonds, whereas the other had both its N-Hs free. Independent verification of H-bond formation was readily obtained by

(21) (a) Bonzli, P.; Gerig, J. T. *J. Am. Chem. Soc.* **1990**, *112*, 3719–3726. (b) Kessler, H.; Will, M.; Antel, J.; Beck, H.; Sheldrick, G. M. *Helv. Chim. Acta* **1989**, *72*, 530–555. (c) Inman, W.; Crews, P. *J. Am. Chem. Soc.* **1989**, *111*, 2822–2889. (d) Kessler, H.; Bats, J. W.; Lautz, J.; Müller, A. *Liebigs Ann. Chem.* **1983**, 913–928. (e) DiBlasio, B.; Rossi, F.; Benedetti, E.; Pavone, V.; Pedone, C.; Temussi, P. A.; Zanotti, G.; Tancredi, T. *J. Am. Chem. Soc.* **1989**, *111*, 9089–9098.

(22) Stevens, E. S.; Sugawara, N.; Bonora, G. M.; Tooniolo, C. *J. Am. Chem. Soc.* **1980**, *102*, 7048–7050.

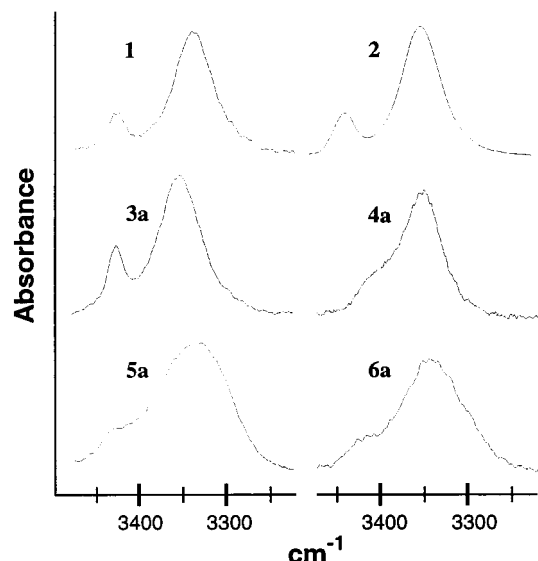


Figure 3. Representative FT-IR spectral data from the N-H stretch region of the templates (3 mM) in CHCl_3 at 298 K. Each spectrum had its baseline corrected, and the absorbance of CHCl_3 was subtracted. Bands at 3410–3450 cm^{-1} are assigned to non-H-bonded N-H stretching, and bands at 3300–3360 cm^{-1} are assigned to an intramolecular, H-bonded N-H stretching. The following maxima were found: template **1**, 3441 and 3341 cm^{-1} ; **2**, 3435 and 3341 cm^{-1} ; **3a**, 3441 and 3341 cm^{-1} ; **4a**, 3414 and 3350 cm^{-1} ; **5a**, 3420 and 3358 cm^{-1} ; **6a**, 3440 and 3357 cm^{-1} .

examining the N-H stretching regions of FT-IR spectra. These spectra showed absorption bands that correspond to H-bonded N-Hs and to free N-Hs (Figure 3).²³ The same relative intensity of these bands was obtained upon diluting the samples to a 1 mM concentration, which is expected if the H-bonds are intramolecular. Furthermore, no significant changes occurred in the width of the N-H signals with changes in concentration of the templates (e.g., template **3a** 100 to 1 mM).

Experimental Structures. Template structures were investigated using NMR analysis. COSY,^{24,25} DQF-COSY,²⁶ NOESY,²⁷ TOCSY,²⁸ and ROESY²⁹ experiments were performed to assign the protons of the templates and to identify protons that are held close together. A general NOE-pattern existed for the templates, which is reasonable considering that the bicyclic aromatic template is rigid and there are a limited number of conformations available for H-bonded amino acids. For amino acids that formed H-bonds, their internal N-Me had NOE's to the protons of the template's bicyclic ring,

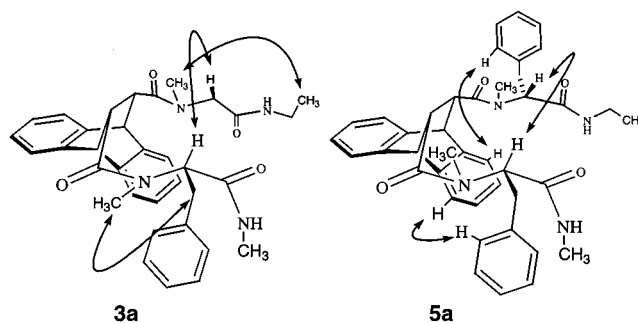


Figure 4. Close proximity of some key hydrogen atoms in templates **3a** and **5a** indicated by the double-headed arrows. Template **3a** had a weak NOE between the α -protons, whereas no association of the side chains was observed in template **2**. Extending the hydrophobic core further in template **5a** resulted in a greater alignment of the side chains with strong NOE's being observed between the α -protons and between protons on the phenyl side chains to the aromatic base of the template.

whereas non-H-bonded amino acids had relatively few NOE's. If NOE's existed for non-H-bonded amino acids, they were between the internal N-Me and the external N-Me of the non-H-bonded amino acid. Templates **4a** and **5a** had an additional NOE between their α -protons. Template **5a** also had NOE's between the phenyl side chains and the aromatic ring of the template.

Bicyclooctene-based template **1**, which does not have an aromatic ring, produced the strongest H-bond in chloroform, according to its temperature coefficient of -7.2 ppb/K (Table 1). Placing a phenyl ring below the H-bonding plane, giving template **2**, did not produce a more stable H-bond as evident by its less negative temperature coefficient (-6.2 ppb/K versus -7.2 ppb/K). Template **1** had a NOE between its internal N-Me's, whereas this signal was not observed for template **2**. Apparently, unfavorable interactions between the aromatic ring and the internal N-Me group of template **2** force the amino acids into a less favorable H-bonding geometry.

To develop a more extensive aromatic cluster, the glycines of template **2** were replaced with phenylalanines. We envisaged that interactions between the aromatic rings of the phenylalanine(s) and the template would help align the amino acids to provide a more stable H-bond. The addition of a single L-phenylalanine did not appear to stabilize an H-bond. One diastereomer, template **3a**, had a more positive temperature coefficient (-5.3 ppb/K) than templates **1** and **2**. On the other hand, template **3a** had a weak NOE between the α -protons of the amino acids (Figure 4). Even though the H-bond strength appears to be enthalpically weaker for template **3a**, the existence of this NOE suggests that interactions between the aromatic rings produced a thermodynamically more stable structure.

The chemical shift of the phenylalanine's α -proton of template **3a** is consistent with its aromatic ring being held near the template's aromatic ring (Figures 4 and 5). Its resonance of 5.4 ppm is downfield from the α -proton of N-Boc N-methyl phenylalanine amide (4.8 ppm in CDCl_3), showing that the proton resides in the deshielding region of the template's aromatic ring. On the other hand, the chemical shift of the α -proton of template **3b** was less deshielded (5.1 ppm). Thus, the arrangement of the phenylalanines in templates **3a** and

(23) Gellman, S. H.; Dado, G. P.; Liang, G.-B.; Adams, B. R. *J. Am. Chem. Soc.* **1991**, *113*, 1164–1173.

(24) Kessler, H.; Bermel, W.; Muller, A.; Pook, K. H. In *The Peptides*; Underfriend, S.; Meinhofer, J., Eds.; Academic Press: London, 1985; Vol. 7, pp 438–473.

(25) (a) *Biomolecular NMR Spectroscopy*; Evans, J. N. S., Ed.; Oxford University Press: Oxford, 1995; Chapter 4. (b) Dyson, H. J.; Wright, P. E. *Annu. Rev. Biophys. Chem.* **1991**, *20*, 519–538. (c) Deber, C. M.; Madison, V.; Blout, E. R. *Acc. Chem. Res.* **1976**, *9*, 106–109. (d) Bystrov, V. F.; Portnova, S. L.; Balashova, T. A.; Koz'min, S. A.; Gavrilov, Yu. D.; Afanas'ev, V. A. *Pure Appl. Chem.* **1973**, *36*, 19–25.

(26) Rance, M.; Sorensen, O. W.; Bodenhausen, G.; Wagner, G.; Ernst, R. R.; Wulthrich, K. *Biochem. Biophys. Res. Commun.* **1983**, *117*, 479–485.

(27) Macura, S.; Ernst, R. R. *Mol. Phys.*, **1979**, *41*, 91–101.

(28) (a) Davis, D. G.; Bax, A. *J. Am. Chem. Soc.* **1985**, *107*, 2820–2827. (b) Braunschweiler, L.; Ernst, R. R. *J. Magn. Reson.* **1983**, *53*, 521–528.

(29) Bax, A.; Davis, D. G. *J. Magn. Reson.* **1985**, *63*, 207–213.

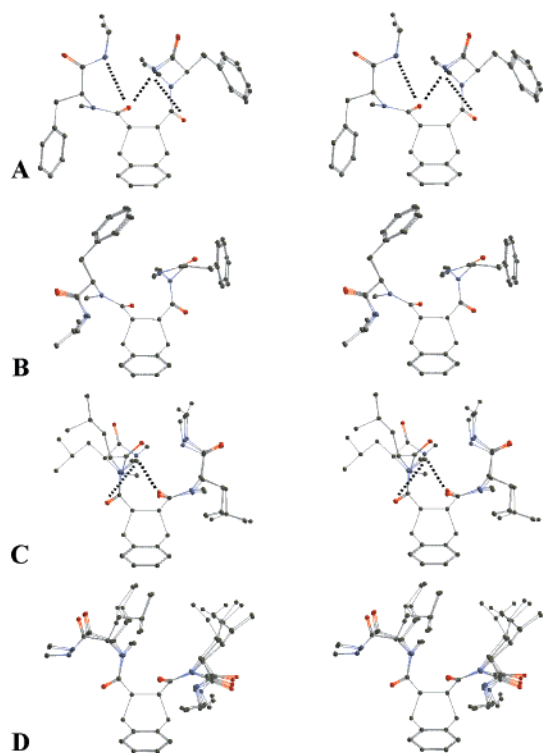


Figure 5. Overlay of lowest energy conformers (within 1 kcal/mol of the global minimum) of the templates, according to a Monte Carlo search procedure. Structures that had the position of the side chains reversed were not included to simplify the figure. The set of higher energy structures within the cut off range were used (the sets were generally defined by either the N-Et or N-Me amide forming the bifurcated H-bond). Dotted lines indicate H-bonds that are consistent with the experimental results. The templates include (A) template **5a** with 6 out of 10 structures overlaid, (B) template **5b** with 7 out of 10 structures overlaid, (C) template **6a** with 3 out of 6 structures overlaid, and finally, (D) template **6b** with 5 out of 10 structures overlaid.

3b depends strongly on their chirality. Template **3b** had only two weak H-bonds and relatively few NOE's. For the rest of the template series, the chemical shift of the α -proton for an H-bonded phenylalanine was significantly downfield compared to the α -proton of *N*-Boc *N*-methyl phenylalanine amide, and thus, they were held near the template's aromatic ring.

A greater dependence of H-bond strength with template structure was observed when both glycines were replaced with L- or D-phenylalanine. As seen with the other templates, templates **4a** and **4b** had only a single H-bond, whereas templates **5a** and **5b** had two and no H-bonds, respectively. Thus, H-bond formation depended on the chirality of the template with the phenylalanines being either properly or improperly aligned to support H-bond formation. Templates **4a** and **4b** composed of two L-phenylalanines had both types of side chains. The internal N-Me of the phenylalanine that is H-bonded had NOE's to the top and bridgehead C-H protons of the template, which is consistent with the H-bond existing over the template (see modeled structures, Figure 5). For the improperly aligned phenylalanine, there was only coupling between one benzylic proton and its internal N-Me. Templates containing a D- and L-phenylalanine provided two diastereomers. One phenylalanine of template **5a** also appears to form an H-bond over the top of

the template, having NOE's between the internal N-Me and the bridgehead proton. But in template **5a**, the other phenylalanine was also properly aligned and formed an isoenergetic H-bond, according to the temperature coefficients. The internal N-Me for this side chain had NOE's to its bridgehead proton as well. A more intense NOE was observed between the α -protons of template **5a** than template **3a**. Most importantly, there existed strong NOE's between both phenyl rings and the ortho protons of the template's aromatic base (Figure 4), which indicates that the rings of template **5a** are associated. The other template, **5b**, which did not have an H-bond, had very little structure, according to its NOESY spectrum.

Theoretical Structures. A search of the conformational space of the templates was performed using both a Monte Carlo method (MMFF94 force field as presented by Spartan Pro) and a manual search procedure (AMBER force field as presented by HyperChem). Global minima from these calculations were consistent for each template. These studies also showed that all structural elements: side chains, aromatic template, and alkyl groups on the internal and external amides, establish a template's structure. Although we wanted to just reduce the number of possible H-bonded structures by methylating the internal amides, the addition of these alkyl groups drastically altered template structure. Steric interactions forced the methyl groups to reside above and away from the template, which placed one internal carbonyl oxygen atom into the H-bonding plane. Alignment of dipole moments forced the other internal carbonyl away from the H-bonding plane (Figure 5).

For most templates, one N-H formed a bifurcated H-bond with the two internal carbonyl oxygen atoms in 10- and 7-membered H-bonded rings, whereas the other N-H formed either a 10- or 7-membered H-bonded ring. According to NMR data, most templates had only one H-bond, and it is most likely this bifurcated one. One possible reason for a single H-bond was that the ethyl amides are too large to be positioned properly. While this assumption seems reasonable, especially considering that the amino acid that is *N*-methylated generally formed the H-bond, molecular modeling results showed that replacing a methyl for an ethyl group gave only a small energy difference. Furthermore, templates **4a** and **4b** have the same temperature coefficient, even though one diastereomer formed an H-bond with the N-H of its ethyl amide and the other with the N-H of its methyl amide. The more likely reason for a single H-bond is that only the bifurcated H-bond is strong enough to form in chloroform, whereas the other potential H-bond is too weak to form unless there are additional favorable interactions between a side chain and the template.

According to the modeling results, both templates **5a** and **5b** should be able to form a strong bifurcated H-bond. Template **5b** had roughly the same H-bonding pattern ((N-)H \cdots O(=C)_{10-member} = 1.8 Å and 158°; (N-)H \cdots O(=C)_{7-member} = 2.9 Å and 105°) as template **5a** ((N-)H \cdots O(=C)_{10-member} = 1.9 Å and 137°; (N-)H \cdots O(=C)_{7-member} = 2.3 Å and 138°). These asymmetrical, bifurcated H-bonds are consistent with experimental results that showed polyalkyl diamides preferentially formed a 10-membered H-bonded ring²³ but contradict results from molecular simulations using the AMBER force field that showed smaller rings were preferred.³⁰ In our studies, calculations using both AMBER and the MMFF94 force

field gave the same lowest energy structures, albeit the H-bond lengths were slightly longer with the AMBER force field.

The major difference between templates **5a** and **5b** is the arrangement of the aromatic rings (Figure 5). In template **5a**, one aromatic side chain has a nearly perpendicular alignment (T-stacked) with the aromatic ring of the template. A centroid distance of 5.5 Å separates these rings, which matches the distance most commonly observed for T-stacked aromatic rings in proteins.^{5a} The other aromatic side chain appears to be positioned too far away from the template's aromatic ring to interact strongly. In template **5b**, both aromatic side chains are positioned far away from the template's aromatic ring. The conformer distributions of both template **5a** and **5b** showed that they are very rigid. For each template, 90% of the conformers at 300 K had only subtle differences in their structures. Half of the conformers had the aromatic side chains arranged as shown in Figure 5, and the other half had the same structures except that the phenylalanine rings, distinguishable by being either an *N*-methyl or *N*-ethyl amide, were switched. Having the *N*-ethyl amide forming the bifurcated H-bond gave a slightly less stable set of conformers ($\Delta\Delta G^\circ < 0.1$ kcal/mol). Because a single conformer was observed for each template in the NMR experiments, the calculated conformers, if they exist, must be interconverting at a rate faster than the NMR time scale. Molecular dynamics simulations, however, showed that the H-bonded structures are not labile at 300 K. The two H-bonds in template **5a** and the lack of an H-bond in template **5b** strongly suggests that aromatic rings have to have a specific arrangement within a hydrophobic core to give enough structure to provide function.

A comparison of the differences in the H-bond strengths (Table 1) and the structures of the templates, as determined by NMR and computational analysis, shows that the nature of the side chain controls the template's structure and function (H-bonding). Adding aromatic rings can enhance structure, but harm function, e.g., template **3a** versus template **1** or enhance both structure and function, e.g., template **5a** compared to template **5b**.

The question remains as to whether aliphatic side chains can enhance a core's structure and function to the same extent as aromatic side chains. Templates **6a** and **6b**, which contain D- and L-leucines, were studied to explicitly compare aromatic–aromatic interactions with aliphatic–aromatic interactions. Template **6a** formed a single bifurcated H-bond, whereas template **6b** had no H-bonds. Both templates had very little structure according to NMR analysis; there were no NOE's between the side chains or between the side chains and the aromatic ring of the template. The lower energy conformations (90% of conformers at 300 K) of these templates (Figure 5) indicate that they are less rigid than templates **5a** and **5b**, especially template **6b**. The calculated lowest energy structure of template **6a** is very similar to the one obtained for template **5a**. The isobutyl side chains of leucine and the benzyl side chains of phenylalanine can be swapped without a major change in template structure.

Experimental results, however, show that the side chains of leucine and phenylalanine are not equivalent in the mimetic cores. Template **5a**, containing two

phenylalanines, forms two H-bonds in chloroform, whereas template **6a**, with two leucines, forms only one H-bond. We cannot state that the slightly stronger H-bond observed in template **5a**, as compared to template **6a** (temperature coefficients of -6.4 and -5.7 ppb/K, respectively) is a result of more favorable aromatic interactions. Template **6a** could be less stable because of greater steric constraints imposed upon aligning the aliphatic side chains for H-bond formation. Another possibility is that the H-bonds of template **5a** interact in a cooperative manner, giving it greater structural stability. The second, unique H-bond observed in template **5a** suggests strongly that aromatic interactions are more stabilizing than aliphatic–aromatic interactions. According to the calculated structure, which is consistent with the observed NOE's, this H-bond exists in a seven-membered ring ((N–)H \cdots O(=C)_{7-member} = 2.3 Å and 138°). A seven-membered ring is available for the other templates as well, but apparently only side chains that can interact favorably with the template's aromatic ring can form one.

For these mimetic cores, aromatic interactions provide for more structure and function than aliphatic–aromatic interactions. We do not know whether the advantage provided by aromatic–aromatic interactions results from a more favorable change in enthalpy or whether the alignment of aliphatic side chains suffer from a greater loss of freedom compared to aromatic side chains.³¹ Molecular dynamics calculations showed that the Leu side chains of template **6a** still had extensive freedom of motion when H-bonded. Therefore, it appears that the entropic loss suffered by the leucine side chains is small, and the driving force for dual H-bond formation in template **5a** results from additional energy provided by T-stacked aromatic rings that is not available to aliphatic–aromatic interactions.

Conclusion

We have demonstrated that simple, synthetic cores composed of aromatic rings and aliphatic groups can be constructed to support H-bond formation between amino acids in a nonaqueous environment. The properties of the core are sensitive to both the arrangement and nature of the side chains. Aromatic rings can provide for more structure and greater function, but if they are not positioned correctly, no structure or function will be obtained. Although most templates had a single H-bond, template **5a**, having three aromatic rings in the core with one pair being apparently held in a T-stacked arrangement, produced two isoenergetic H-bonds. Amino acids containing H-atoms or aliphatic side chains held in a similar position as the T-stacked aromatic side chain did not form an H-bond. These templates place the aliphatic side chain of leucine at the edge of an aromatic ring, whereas Wilcox's molecular torsional balance¹² placed aliphatic groups at the face of aromatic rings. Combining our results with those of Wilcox suggests that aliphatic groups are as stabilizing as aromatic groups when they are held at the face of an aromatic ring, but not when they are placed at the aromatic edge.

Experimental Section

General Experimental Procedures. NMR spectra used for conformational analysis were measured in CDCl₃ using a Bruker AMX400 spectrometer operating at 400.14 MHz for

(30) McDonald, D. Q.; Still, W. C. *J. Am. Chem. Soc.* **1994**, *116*, 11550–11553.

(31) (a) Pal, D.; Chakrabarti, P. *Proteins* **1999**, *36*, 332–339. (b) Doig, A. J. *Biophys. Chem.* **1996**, *61*, 131–141.

proton and a Bruker AC250 operating at 62.9 MHz for carbon nuclei. Chemical shifts are in ppm and are referenced using an internal TMS standard. The following are typical of the parameters used in the NMR studies: NOESY were obtained at 298 K; mixing time = 150 and 300 ms; and FID acquisition time was 0.15 s. Other parameters were SW = 5800 Hz, 2 K data points and 256 or 512 increments each with 16 transients per FID. TOCSY experiments were run with a 300 ms mixing time, L1 = 118 and low power pulse = 15 dB. ROESY experiments were obtained at 298 K with a cw pulse power of 30 dB and a mixing time of 400 ms. A QSINE window function was applied in both dimensions with ssb = 2, and the data was phased in the usual fashion. Homonuclear proton–proton decoupling experiments were run on the Bruker AC250 operating at 249.99 MHz.

Establishment of relative NOE strengths of the α -proton– α -proton cross-peaks for templates **4a** and **5a** was accomplished by first setting the NOE intensities of the cross-peaks between the benzylic and α -protons of these templates to a constant value. This NOE was chosen as a standard because it was separated from other signals and interaction strength between these protons should be approximately equivalent in both templates. Peak areas for the α -proton– α -proton NOE's were then integrated. We found that this area was three times larger for template **5a** than **4a**.

All syntheses were carried out under positive argon pressure, and DMF was freshly distilled under vacuum over MgSO_4 . K_2CO_3 was powdered and dried under vacuum for 1 h prior to use. All other solvents and reagents were used as purchased. A MEL-TEMP (Laboratory Devices) apparatus was used to determine the melting points of the compounds; these values are given uncorrected. HPLC analysis was performed on a Shimadzu 10A series HPLC using a C_{18} reversed-phase column and water/ CH_3CN as the eluent. UV–vis titrations were performed on a Hewlett-Packard Kayak XA series spectrophotometer. Water for the HPLC assays was purified on a Millipore water purification system. Abbreviations: PyBOP, benzotriazol-1-yloxy-tripyrrolidinophosphonium hexafluorophosphate.

Calculated Structural Determination Global minimum structures of the templates were determined through a Monte Carlo search method using the MMFF94 force field (package procedure of SpartanPro).^{32a} Generally, over 1500 structures were created and analyzed for potential energy through a simulated annealing process starting at 5000 K and ending at 300 K. Molecular dynamics simulations were also performed using the AMBER force field as presented by Hyperchem.^{32b} A series of compounds were generated for each template by heating them to 800 K. At this temperature, the H-bonds were periodically broken and the side chains could swap their positions, i.e., above and away from the base of the template or closer to the template. A total simulation time of 5 ps was used with 1 fs steps. Random conformers were chosen (ca. 20) during the simulation process and minimized using the Polak-Ribiere minimization algorithm (RMS gradient of 0.005 kcal/(Å mol)). Most compounds minimized to a single conformer that was over 1 kcal/mol lower in energy than the other minimized structures. This procedure was used for templates **5a,b** and **6a,b**, and their lowest energy conformers for each template matched the ones obtained from the Monte Carlo search.

Disarcosine Methyl/Ethyl Amide (1). To a solution of bicyclo[2.2.2]oct-5-ene-2,3-dicarboxylic acid¹⁶ (187 mg, 1.05 mmol) in DMF (5 mL) were added sarcosine methyl amide trifluoroacetate (227 mg, 1.05 mmol) and K_2CO_3 (152 mg, 1.10 mmol). After the mixture was stirred for 1 h at room temperature, DIEA (0.18 mL, 1.05 mmol) and PyBOP (546 mg, 1.05 mmol) were added. After the reaction mixture became transparent (ca. 10 min), sarcosine ethyl amide trifluoroacetate (253 mg, 1.10 mmol) and an additional equivalent of K_2CO_3 (152 mg, 1.10 mmol) were added, and the solution was stirred overnight. The reaction mixture was concentrated in vacuo to

remove DMF, dissolved in EtOAc (50 mL), and extracted with 5% NaHCO_3 (10 mL), 5% HCl (10 mL), and brine (20 mL). The organic layers were combined and concentrated, and the crude material was separated via HPLC purification. Template **1** was obtained as a white solid (225 mg, 57%) (R_f = 0.47, 10% MeOH in CHCl_3). Mp: 132–133 °C. ^1H NMR (400 MHz, CDCl_3) δ : 6.81 (bq, 1 H), 6.53 (t, J = 7.2 Hz, 1 H), 6.26 (bt, 1 H), 6.25 (t, J = 7.3 Hz, 1 H), 4.54 (d, J = 16.2 Hz, 1 H), 4.31 (d, J = 15.8 Hz, 1 H), 3.70 (d, J = 15.7 Hz, 1 H), 3.47 (d, J = 16.2 Hz, 1 H), 3.33 (dd, J = 1.4, 10.1 Hz, 1 H), 3.24 (m, 1 H), 3.21 (m, 1 H), 3.09 (m, 1 H), 2.99 (s, 3 H), 2.91 (m, 1 H), 2.87 (m, 1 H), 2.72 (d, J = 4.7 Hz, 3 H), 1.59 (m, 2 H), 1.41 (m, 2 H), 1.12 (t, J = 7.3, 3 H). ^{13}C NMR (63 MHz, CDCl_3) δ : 173.8, 173.6, 169.3, 168.0, 133.9, 130.5, 57.2, 52.0, 47.3, 46.7, 35.9, 34.4, 33.6, 33.1, 26.0, 25.2, 24.6, 14.8. HRMS m/z calcd for $\text{C}_{19}\text{H}_{30}\text{N}_4\text{O}_4$ (MNa^+) 401.2159, found 401.2122.

Disarcosine Methyl/Ethyl Amide (2). Powdered K_2CO_3 (289 mg, 2.09 mmol) was added to a solution of sarcosine methyl amide trifluoroacetate (411 mg, 1.90 mmol) and 9,10-dihydro-9,10-ethanoanthracene-11,12-dicarboxylic acid anhydride¹⁵ (525 mg, 1.90 mmol) in DMF (8 mL). After the mixture was stirred for 1 h at room temperature, DIEA (0.33 mL, 1.90 mmol) and PyBOP (989 mg, 1.90 mmol) were added. Once the reaction mixture became transparent (ca. 10 min), sarcosine ethyl amide trifluoroacetate (437 mg, 1.90 mmol) and K_2CO_3 (289 mg, 2.09 mmol) were added, and the solution was stirred overnight. The reaction mixture was concentrated in vacuo and dissolved in EtOAc. Insoluble impurities were removed via vacuum filtration. The filtrate was precipitated by adding Et_2O , and the resulting solid material was subjected to HPLC purification. Template **2** was obtained as a pale yellow solid (R_f = 0.4, 10% MeOH in CHCl_3), 200 mg (22%). Mp: 159–160 °C. ^1H NMR (400 MHz, CDCl_3) δ : 7.14–7.33 (m, 8 H), 6.53 (bq, 1 H), 6.20 (bt, 1 H), 4.63 (d, J = 1.6 Hz, 1 H), 4.57 (d, J = 1.8 Hz, 1 H), 4.31 (d, J = 15.6 Hz, 1 H), 4.09 (d, J = 15.6 Hz, 1 H), 3.72 (d, J = 15.8 Hz, 1 H), 3.59 (d, J = 15.6 Hz, 1 H), 3.49 (m, 2 H), 3.29 (dd, J = 2.0, 10.1 Hz, 1 H), 3.21 (m, 1 H), 3.16 (s, 3 H), 3.02 (s, 3 H), 2.66 (d, J = 4.8 Hz, 3 H), 1.06 (t, J = 7.3 Hz, 3 H). ^{13}C NMR δ : 172.2, 169.2, 168.1, 143.2, 142.7, 140.8, 140.1, 126.6, 126.1, 125.7, 125.0, 123.5, 52.3, 52.1, 47.1, 46.4, 36.8, 36.2, 34.3, 25.9, 14.6. HRMS m/z calcd for $\text{C}_{27}\text{H}_{32}\text{N}_4\text{O}_4$ (M^+) 476.2423, found 476.2396.

Sarcosine Ethyl/*N*-Methyl *L*-Phenylalanine Methyl Diamide (3a,b). A solution of *N*-methyl-*L*-phenylalanine methyl amide trifluoroacetate (579 mg, 1.9 mmol), 9,10-dihydro-9,10-ethanoanthracene-11,12-dicarboxylic acid anhydride¹⁵ (497 mg, 1.8 mmol) and K_2CO_3 (274 mg, 2.0 mmol) in DMF (8 mL) was allowed to stir for 18 h, at which time DIEA (0.33 mL, 1.9 mmol) and PyBOP (989 mg, 1.9 mmol) were added. After the solution was mixed for 20 min, sarcosine ethyl amide trifluoroacetate (437 mg, 1.9 mmol) and K_2CO_3 (274 mg, 1.9 mmol) were added, and the reaction mixture was stirred overnight. Concentrating the crude material in vacuo produced an oil, which was dissolved in EtOAc (150 mL) and extracted with H_2O (3 \times 10 mL) and brine (20 mL). The organic layers were collected, dried over MgSO_4 , concentrated in vacuo, and then subjected to HPLC purification. The diastereomers **3a** and **3b** were separated, giving 110 mg (11%) of each as white solids. **3a** (R_f = 0.47, 10% MeOH in CHCl_3). Mp: 145–146 °C. ^1H NMR (400 MHz, CDCl_3) δ : 7.34–7.06 (m, 13 H), 6.39 (bq, 1 H), 6.15 (bt, 1 H), 5.4 (m, 1 H), 4.53 (d, J = 1.7 Hz, 1 H), 4.23 (d, J = 1.5 Hz, 1 H), 3.89 (d, J = 15.1 Hz, 1 H), 3.80 (d, J = 15.1 Hz, 1 H), 3.36 (m, 1 H), 3.32 (m, 1 H), 3.22 (m, 1 H), 3.19 (m, 1 H), 3.06 (m, 1 H), 2.93 (m, 1 H), 2.82 (s, 3 H), 2.63 (d, J = 4.7 Hz, 3 H), 1.06 (t, J = 7.2 Hz, 3 H). ^{13}C NMR (63 MHz, CDCl_3) δ : 172.1, 172.0, 170.5, 168.1, 143.1, 142.7, 140.5, 139.7, 137.4, 128.7, 128.3, 126.4, 126.3, 126.2, 125.8, 125.6, 125.4, 124.8, 123.3, 56.5, 51.8, 47.2, 46.3, 36.4, 34.3, 34.0, 25.9, 14.4. HRMS m/z calcd for $\text{C}_{34}\text{H}_{38}\text{N}_4\text{O}_4$ (MNa^+) 589.2785, found 589.2670. **3b** (R_f = 0.51, 10% MeOH in CHCl_3). Mp: 150–151 °C. ^1H NMR (400 MHz, CDCl_3) δ : 7.60–6.99 (m, 13 H), 6.58 (bt, 1 H), 5.98 (bq, 1 H), 5.12 (m, 1 H), 4.69 (d, J = 1.8 Hz, 1 H), 4.39 (d, J = 1.8 Hz, 1 H), 3.99 (d, J = 15.9 Hz, 1 H), 3.48 (m, 1 H), 3.47 (m, 1 H), 3.29 (m, 1 H), 3.23 (s, 3 H), 3.15 (m, 1 H), 3.11 (m, 1 H), 2.89 (d, J = 10.0 Hz, 1 H), 2.84 (d, J = 4.8

(32) (a) Wavefunction, Inc., Irvine, CA. (b) Hypercube, Inc., Gainesville, FL.

Hz, 3 H), 2.13 (s, 3 H), 1.07 (t, $J = 7.3$ Hz, 3 H). ^{13}C NMR (63 MHz, CDCl_3) δ : 172.2, 171.5, 170.2, 168.6, 143.7, 141.7, 141.4, 139.3, 137.0, 129.1, 128.9, 128.7, 128.6, 126.8, 126.7, 126.5, 126.3, 126.1, 124.9, 123.5, 123.4, 123.2, 57.4, 52.7, 47.1, 46.5, 46.4, 35.0, 34.2, 33.0, 31.2, 25.9, 14.3. HRMS m/z : calcd for $\text{C}_{34}\text{H}_{38}\text{N}_4\text{O}_4$ (MNa^+) 589.2785, found 589.2821.

Di-*N*-methyl-L-phenylalanine Methyl/Ethyl Amide (4a,b). A solution of 9,10-dihydro-9,10-ethanoanthracene-11,12-dicarboxylic acid anhydride¹⁵ (530 mg, 1.92 mmol), *N*-methyl-L-phenylalanine ethyl amide trifluoroacetate (619 mg, 2.02 mmol), and K_2CO_3 (319 mg, 2.31 mmol) in DMF (5 mL) was allowed to stir for 18 h, after which time PyBOP (1.0 g, 1.92 mmol) and DIEA (0.37 mL, 2.12 mmol) were added. Once the solution became transparent (ca. 10 min), *N*-methyl-L-phenylalanine methyl amide trifluoroacetate (590 mg, 2.02 mmol) and K_2CO_3 (319 mg, 2.31 mmol) were added, and the solution was allowed to stir overnight. After the reaction mixture was concentrated in vacuo, the resulting oil was dissolved in EtOAc (150 mL), extracted with H_2O (3×10 mL) and then brine (20 mL), dried (MgSO_4), concentrated in vacuo, and subjected to HPLC purification. The diastereomers **4a** and **4b** were separated, giving 145 mg (12%) of **4a** and 105 mg (8%) of **4b** as white solids. **4a** ($R_f = 0.33$, 10% MeOH in CHCl_3). Mp: 145–146 °C. ^1H NMR (400 MHz, CDCl_3) δ : 7.04–7.48 (m, 18 H), 6.25 (bt, 1 H), 6.07 (bq, 1 H), 5.47 (dd, $J = 4.4$, 6.0 Hz, 1 H), 4.90 (dd, $J = 4.4$, 6.0 Hz, 1 H), 4.42 (d, $J = 1.5$ Hz, 1 H), 4.32 (d, $J = 1.5$ Hz, 1 H), 3.38 (m, 1 H), 3.34 (m, 1 H), 3.28 (m, 1 H), 3.24 (m, 1 H), 3.06 (s, 3 H), 3.03 (m, 1 H), 2.88 (m, 1 H), 2.86 (m, 1 H), 2.75 (d, $J = 4.8$ Hz, 3 H), 2.75 (m, 1 H), 2.34 (s, 3 H), 0.95 (s, 3 H). ^{13}C NMR (as mixture of diastereomers) (63 MHz, CDCl_3) δ : 172.1, 171.8, 171.6, 170.8, 141.2, 138.6, 136.2, 128.7, 128.6, 128.4, 126.5, 126.4, 125.3, 125.1, 124.8, 124.6, 124.1, 123.6, 122.6, 60.1, 59.8, 58.4, 57.2, 57.1, 56.0, 41.2, 40.6, 32.9, 31.8, 29.0, 16.1, 15.8. HRMS m/z : calcd for $\text{C}_{41}\text{H}_{44}\text{N}_4\text{O}_4$ (MNa^+) 679.3255, found 679.3267. **4b** ($R_f = 0.46$, 10% MeOH in CHCl_3). Mp: 139–140 °C. ^1H NMR (400 MHz, CDCl_3) δ : 7.31–7.04 (m, 18 H), 6.43 (bq, 1 H), 5.97 (bt, 1 H), 5.55 (dd, $J = 4.2$, 5.8 Hz, 1 H), 4.91 (dd, $J = 4.2$, 5.8 Hz, 1 H), 4.41 (s, 1 H), 4.37 (s, 1 H), 3.48 (m, 1 H), 3.43 (m, 1 H), 3.34 (m, 1 H), 3.22 (m, 1 H), 3.12 (m, 1 H), 3.04 (m, 1 H), 2.81 (dd, $J = 11.7$, 15.3 Hz, 1 H), 2.66 (d, $J = 4.5$ Hz, 1 H), 2.62 (d, $J = 10$ Hz, 1 H), 2.10 (s, 3 H), 1.09 (t, $J = 7.3$ Hz, 3 H). HRMS m/z : calcd for $\text{C}_{41}\text{H}_{44}\text{N}_4\text{O}_4$ (MNa^+) 679.3255, found 679.3284.

Di-*N*-methyl-D/L-phenylalanine Methyl/Ethyl Amide (5a,b). Synthesis and workup followed the procedure outlined for the synthesis of compound **4**, except the first amino acid added was *N*-methyl-D-phenylalanine methyl amide and the reaction scale was 0.7 mmol of amino acid. The diastereomers **5a** and **5b** were separated, giving 40 mg (9%) and 80 mg (18%), respectively, as white solids. **5a** ($R_f = 0.37$, 10% MeOH in CHCl_3). Mp: 260 °C dec. ^1H NMR (400 MHz, CDCl_3) δ : 7.33 (m, 1H), 7.32 (m, 1H), 7.31 (m, 2H), 7.30 (m, 2H), 7.23 (m, 2H), 7.22 (m, 2H), 7.21 (m, 2H), 7.10 (m, 2H), 6.99 (m, 2H), 6.91 (m, 2H), 6.59 (bq, 1 H), 6.41 (bt, 1 H), 5.33 (dd, $J = 7.4$, 7.4 Hz, 1 H), 5.20 (dd, $J = 7.9$, 7.9 Hz, 1 H), 4.28 (s, 1 H), 4.25 (s, 1 H), 3.27 (m, 1 H), 3.24 (m, 1 H), 3.20 (m, 1 H), 3.14 (m, 1 H), 3.10 (m, 1 H), 3.08 (m, 1 H), 2.91 (s, 3 H), 2.89 (m, 1 H), 2.87 (s, 3 H), 2.86 (m, 1 H), 2.62 (d, $J = 4.6$ Hz, 3 H), 0.96 (t,

$J = 7.0$ Hz, 3 H). ^{13}C NMR (63 MHz, CDCl_3) δ : 171.7, 171.6, 170.4, 169.4, 137.4, 137.2, 128.9, 128.6, 128.5, 126.7, 126.5, 125.6, 125.4, 125.3, 123.4, 56.7, 56.2, 47.2, 46.7, 34.6, 34.5, 30.3, 26.1, 14.3. HRMS m/z : calcd for $\text{C}_{41}\text{H}_{44}\text{N}_4\text{O}_4$ (MNa^+) 679.3255, found 679.3309. **5b** ($R_f = 0.50$, 10% MeOH in CHCl_3). Mp: 155–156 °C. ^1H NMR (400 MHz, CDCl_3) δ : 7.3–7.1 (m, 18 H), 6.11 (bs, 2 H), 4.60 (bs 2 H), 4.55 (s, 1 H), 4.49 (s, 1 H), 3.35–2.35 (bm, 17 H), 1.03 (t, $J = 7.2$ Hz, 3 H). ^{13}C NMR (obtained by subtracting **5a** from a mix of diastereomers **5a** and **5b**) (63 MHz, CDCl_3) δ : 172.7, 172.6, 170.3, 170.0, 143.5, 142.4, 141.7, 139.0, 126.8, 126.4, 126.3, 124.1, 123.9, 123.1, 56.6, 56.4, 47.1, 46.9, 33.8, 33.3, 29.2, 26.4, 14.5. HRMS m/z : calcd for $\text{C}_{41}\text{H}_{44}\text{N}_4\text{O}_4$ (MNa^+) 679.3255, found 679.3308.

Di-*N*-methyl-D/L-leucine Methyl/Ethyl Amide (6). Synthesis and workup followed the procedure outlined for the synthesis of compound **4**, except the first amino acid added was *N*-methyl-D-leucine methyl amide, the second was *N*-methyl-L-leucine methyl amide, and the reaction scale was 0.4 mmol of the amino acid. The diastereomers **6a** and **6b** were separated, giving 80 mg (34%) of **6a** and 40 mg (17%) of **6b** as white solids. **6a** ($R_f = 0.57$, 10% MeOH in CHCl_3). Mp: 225 °C dec. ^1H NMR (400 MHz, CDCl_3) δ : 7.30–7.13 (m, 8 H), 6.60 (bq, 1 H), 6.36 (bt, 1 H), 5.03 (dd, $J = 7.8$, 7.8 Hz, 1 H), 4.95 (dd, $J = 7.8$, 7.8 Hz, 1 H), 4.52 (s, 2H), 3.30 (dd, $J = 1.7$, 6.4 Hz, 1 H), 3.29 (d, $J = 6.4$ Hz, 1 H), 3.12 (m, 2 H), 2.82 (s, 6 H), 2.65 (d, $J = 4.8$ Hz, 3 H), 1.61 (m, 2 H), 1.51 (m, 1 H), 1.50 (m, 1 H), 0.97 (m, 6 H), 0.96 (m, 3 H), 0.87 (m, 6 H). ^{13}C NMR (63 MHz, CDCl_3) δ : 172.0, 171.8, 169.8, 168.2, 127.1, 126.8, 126.6, 125.2, 125.0, 61.0, 55.2, 45.0, 42.0, 35.5, 35.0, 26.1, 25.1, 23.1, 22.3, 16.1, 15.6. HRMS m/z : calcd for $\text{C}_{35}\text{H}_{49}\text{N}_4\text{O}_4$ (M^+) 589.3754, found 589.3726. **6b** ($R_f = 0.66$, 10% MeOH in CHCl_3). Mp: 238–240 °C. ^1H NMR (400 MHz, CDCl_3) δ : 6.12 (m, 1 H), 6.11 (m, 1 H), 4.79 (m, 1 H), 4.76 (m, 1 H), 4.55 (s, 1 H), 4.52 (s, 1 H), 3.42 (m, 1 H), 3.32 (m, 1 H), 3.16 (m, 1 H), 3.10 (m, 1 H), 2.96 (s, 3 H), 2.93 (s, 3 H), 2.78 (d, $J = 4.8$ Hz, 3 H), 1.89 (m, 1 H), 1.88 (m, 1 H), 1.42 (m, 2 H), 1.26 (m, 1 H), 1.20 (m, 1 H), 1.13 (t, $J = 7.2$ Hz, 3 H), 0.86 (m, 6 H), 0.85 (m, 6 H). ^{13}C NMR (63 MHz, CDCl_3) δ : 171.5, 171.1, 169.4, 168.5, 126.4, 126.0, 125.8, 125.3, 124.9, 123.5, 54.7, 46.9, 36.8, 36.5, 34.2, 30.8, 25.3, 25.2, 23.0, 22.6, 15.4, 14.8. HRMS m/z : calcd for $\text{C}_{35}\text{H}_{49}\text{N}_4\text{O}_4$ (M^+) 589.3754, found 589.3746.

Acknowledgment. We thank the University of Cincinnati for their generous funding of this project. We also thank Dr. Raghav Yamdagni of the University of Calgary, Alberta, Canada, for his helpful discussions regarding the ROESY experiments performed in this work. J.A.T. was supported by the University of Cincinnati Research Council Fellowship and the Lange Fellowship.

Supporting Information Available: NOESY spectrum and assignment table of template **5a**; plots of changes in chemical shifts of N–H protons with temperature that provided temperature coefficients of Table 1. This material is available free of charge via the Internet at <http://pubs.acs.org>.

JO0106849